Generation of a Precise Roadway Map for Autonomous Cars

Kichun Jo, *Student Member, IEEE*, and Myoungho Sunwoo, *Member, IEEE*

***Abstract*—This paper proposes a map generation algorithm for a precise roadway map designed for autonomous cars. The roadway map generation algorithm is composed of three steps, namely, data acquisition, data processing, and road modeling. In the data acquisition step, raw trajectory and motion data for map generation are acquired through exploration using a probe vehicle equipped with GPS and on-board sensors. The data processing step then processes the acquired trajectory and motion data into roadway geometry data. GPS trajectory data are unsuitable for direct roadway map use by autonomous cars due to signal interruptions and multipath; therefore, motion information from the on-board sensors is applied to refine the GPS trajectory data. A fixed-interval optimal smoothing theory is used for a refinement algorithm that can improve the accuracy, continuity, and reliability of road geometry data. Refined road geometry data are represented into the B-spline road model. A gradual correction algorithm is proposed to accurately represent road geometry with a reduced amount of control parameters. The developed map generation algorithm is verified and evaluated through experimental studies under various road geometry conditions. The results show that the generated roadway map is sufficiently accurate and reliable to utilize for autonomous driving.**

***Index Terms*—Autonomous car, B-spline, optimal smoothing, road map, road modeling.**

I. Introduction

A precise roadway map is fundamental information for driving autonomous cars. This information is the basis for many functions that work in an autonomous car driving system. For example, a roadway network map is the basis for the path routing function that finds the optimal path to reach a destination. Road geometry information of the roadway map is used as a base frame by the on-road navigation algorithm that generates a drivable road path [1], [2]. A localization algorithm can improve the accuracy and reliability of the position estimates through the utilization of prior road geometry information [3]–[6]. A perception algorithm can also increase the performance of detection and classification through the use of road geometry constraints on the map. In addition to the autonomous driving algorithm, a precise roadway map can be utilized for advanced driver assistant system applications such as lane keeping and departure warning systems, fuel efficiency management systems, and intersection safety applications [7]–[9].

There are two major roadway map requirements for autonomous car applications, namely, a *geometry requirement* and an *implementation requirement*. The *geometry requirement* is related to the quality of the roadway map. The data of the roadway map for an autonomous driving application should represent road geometry precisely and accurately. In addition, there must be no fault or discontinuous regions in the roadway map because inaccurate or false representations of road geometry may cause a malfunction of the autonomous driving system. The *implementation requirement* is related to the implementation issues of the roadway map on the autonomous driving system. A roadway map should have an efficient and compact data structure to reduce the data storage of autonomous driving. If the data structure requires a huge amount of memory to represent road geometry, it may require a large data storage and a high-performance database management system that would be impractical for use by the automotive industry. In addition, a compact representation of a road map would enable an efficient online data transfer of road information. Furthermore, if a data structure of a roadway map is designed for easy application to an autonomous driving algorithm (such as perception and planning), it may reduce the computational burden of preprocessing of the road geometry.

This paper presents a data processing and road modeling method for roadway map generation that satisfies the *geometry* and *implementation requirements* of a map for autonomous cars. A probe vehicle equipped with the GPS and on-board sensors are used for roadway map data acquisition. The acquired position and motion data of the probe vehicle are processed using an optimal smoothing technique that satisfies the *geometry requirement*. The optimal smoothing algorithm integrated in the position and motion data from the probe vehicle is based on the Bayesian filter theory that improves the accuracy, continuity, and reliability of the road geometry data for autonomous cars. The *implementation requirement* is satisfied using mathematical road modeling that describes the processed road geometry with a mathematical representation. The B-spline curve is selected for road modeling. Many parameters are required (such as number of knots, knot vectors, and control points) to represent the road geometry with the B-spline.

Manuscript received May 24, 2013; revised September 15, 2013; accepted November 13, 2013. Date of publication December 11, 2013; date of current version May 30, 2014. This work was supported in part by the National Research Foundation grant funded by the Korean government (Ministry of Education, Science and Technology) under Grant 2011-0017495, by the Industrial Strategy Technology Development Program of Ministry of Knowledge Economy (MKE) under Grant 10039673, by the Energy Resource R&D program under Grant 2006ETR11P091C under the Ministry of Knowledge Economy, Science and Technology through the BK21 Program (201000000000173), and by the MKE and Korea Institute for Advancement in Technology (KIAT) through the Workforce Development Program in Strategic Technology. The Associate Editor for this paper was Q. Kong.

The authors are with the Automotive Control and Electronics Laboratory (ACE Lab), Department of Automotive Engineering, Hanyang University, Seoul 133-791, Korea (e-mail: jokihaha@hanyang.ac.kr; msunwoo@hanyang.ac.kr).

Color versions of one or more of the figures in this paper are available online at http://ieeexplore.ieee.org.

Digital Object Identifier 10.1109/TITS.2013.2291395

A gradual correction algorithm is proposed to determine the B-spline parameter suboptimally. The proposed gradual correction algorithm is a simplified algorithm of the dominant points-based B-spline curve fitting algorithm developed in the field of computer-aided design (CAD) research [10]. For the same amounts of control parameters, the proposed gradual correction approach can generate a B-spline road model with high accuracy that is superior to conventional approaches.

This paper is organized as follows. Section II introduces related research work. Section III presents the overall system architecture. Sections IV and V describes data processing with optimal smoothing and a road modeling method with a B-spline road model, respectively. Section VI describes the experimental results and the final section provides conclusions.

II. Related Research

A. Roadway Geometry Data Acquisition and Processing

There have been many studies on how to satisfy the first geometry requirement of a roadway map. Probe vehicles that are equipped with a position measurement system are widely used for roadway data acquisition [7], [11]–[17]. The single GPS receiver is the most widely used for the positioning system of the probe vehicles because it is convenient to equip on vehicles and provides global position of vehicle trajectory. However, data from a single GPS receiver are not perfect to use for the map generation of an autonomous car due to low accuracy and unreliability. A massive database of the trajectories of multiple probe vehicles has been attempted in order to solve the GPS inaccuracy and unreliability problem [12], [16], [17]; however, the generation of a roadway map using this method requires significant road trace data and is too inaccurate to apply to autonomous cars. A real-time kinematic (RTK) GPS and postprocessing kinematic (PPK) GPS can solve the inaccuracy problem of a single GPS receiver because it provides a centimeter-level accuracy using real-time correction and postprocessing [18], [19]. However, the RTK-GPS and PPK-GPS are sensitive to satellite signal conditions. Obstacles, such as tall buildings or tunnels around the GPS receiver, can generate a GPS outage and multiple path. In addition, it can cause discontinuity and unreliability problems for an autonomous driving map.

To address the reliability problem of GPS, many studies have used a sensor fusion algorithm that integrates GPS measurements with data from inertial sensors [7], [20], [21]. The sensor fusion algorithm from previous studies uses a Bayesian filtering-based approach such as the Kalman filter, the extended Kalman filter, and the unscented Kalman filter that use measurement data before the time of a state update. However, map generation is usually performed offline and optimal smoothing techniques that use all the measurement data (before and after) the time of the state update can be applied for map generation [21]. An optimal smoothing based map generation will improve the accuracy and reliability of a roadway map since it uses more data than a filtering approach to estimate roadway geometry.

In addition to the probe vehicle-based map generation approaches, there are many other methods to generate a roadway map, such as laser scanner-based map generation [22], [23] and the processing of an aerial image [24]. However, the focus of this paper is on a probe vehicle-based map generation algorithm.

B. Mathematical Road Modeling

The second requirement related to the implementation of road geometry on an autonomous system can be achieved with mathematical road modeling. Sequential point data from the data acquisition and processing system can be compressed into simple parametric road model equations using mathematical road modeling. In addition, the mathematical representation can be directly applied to the road geometry-based autonomous driving applications.

There are many approaches to model road geometry with a mathematical representation. The discrete polygon is the simplest way to model the road geometry with line segments; however, many line segments are required to achieve the desired accuracy for a roadway map if the road has a large curvature. The combination of straight lines, circles, and clothoids is a traditional design element of a roadway [25]. The clothoid curve is the best way to describe roadway geometry because a curvature linearly varies with its arc length, and it provides smooth steering when passing a curved road. However, although a clothoid curve is the best model to represent road geometry, it is not convenient to utilize for autonomous car applications due to the transcendental function of the clothoid curve [14].

To replace and approximate the clothoid curve representation, a spline curve that consists of sequential curve segments is widely used for road modeling [15], [16], [18], [19], [26]–[29]. The approximation of road geometry with a spline curve is very stable and simple since a spline is composed of linear equations of piecewise curve segments. Furthermore, there are many techniques and tools for the approximation of certain geometry since the spline has been researched for a long time in the field of the CAD/CAM industry.

Two types of spline (interpolating spline and approximating spline) are widely used to construct a road model. The interpolating spline represents a road geometry using control points that are directly passed by a road model [14], [30]. The shape of a road can be intuitively estimated only using control points. Natural cubic spline (cubic Hermite spline) is a representative interpolating spline. The natural cubic spline has an advantage that it can conveniently represent the road model only using waypoints; however, it has a disadvantage in that the change of one control point can affect all shapes of a road model. The approximating spline represents a road geometry by using indirect control points not passed by a road model [13], [16], [28], [29]. B-spline is a representative approximating spline method. Although the B-spline representation is not intuitive due to the indirect control points, local modification of a road model is possible because the change of one control point only affects the small range of road model.

Control points of each spline should be appropriately determined in order to represent the road geometry with the interpolating or approximating spline. Many studies to find control points and spline parameters are concerned with accuracy [13], [16], [28], [29]; however, these studies do not consider the optimization aspect of the number of control points. The

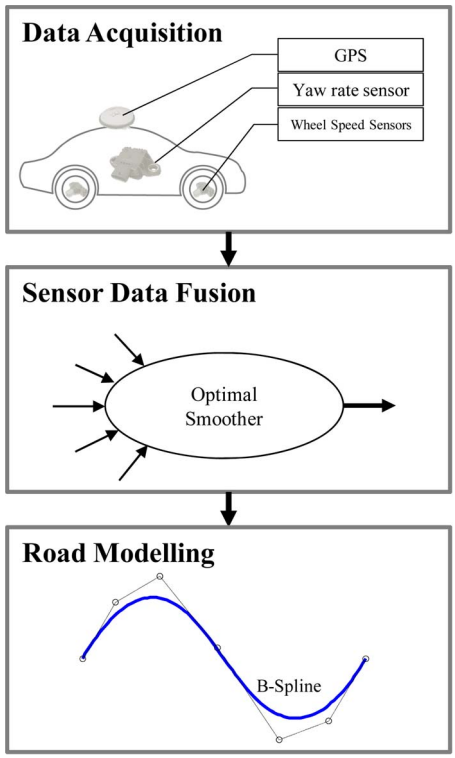

Fig. 1. Road map construction is composed of a three-step process.

number of control points is an important factor to reduce the data storage and improve the map data transfer. Therefore, this study equally focuses on the efficiency and accuracy aspect to represent road geometry through an application of the gradual correction algorithm.

III. System Overview

The overall structure of the road map generation algorithm consists of three steps, namely, data acquisition, data fusion, and road modeling (see Fig. 1). In the first step, raw data for road map generation is acquired by a probe vehicle. In this paper, the probe vehicle is equipped with a RTK-GPS with centimeter-level accuracy under good GPS signal conditions. Other types of GPS (such as PPK-GPS) can be used according to the desired accuracy. The accuracy of the RTK-GPS is sufficient to use for autonomous driving; however, the reliability and continuity of the RTK-GPS cannot satisfy the requirements of a positioning system for autonomous cars because it is too sensitive to external signal conditions, such as the existence of signal obstacles around a vehicle. The vulnerabilities of the GPS system need to be addressed in order to obtain more reliable and continuous position data for the map generation of autonomous cars.

Data fusion with vehicle on-board sensors can be a solution for the vulnerability of GPS. Since the vehicle on-board sensors provide the information about vehicle motion constraints, it is possible to detect GPS malfunctions by verifying that data satisfies the motion constraint. In this paper, two types of vehicle motion sensors (yaw rate gyro and wheel speed) are applied to the data acquisition. Fig. 2 describes the autonomous car A1 used for the probe vehicle of map generation algorithm.

Fig. 2. Autonomous car A1 used for the map generation algorithm.

TABLE I
On-Vehicle Sensor Specifications

Sensor	Frequency	Range	Resolution	Noise (RMS)	Unit
Yaw rate	50 Hz	± 120	0.0625	0.5	deg/sec
Steering angle	50 Hz	± 200	0.006	0.2	deg
Wheel speed	50 Hz	0−130	0.035	0.3	m/s

TABLE II
GPS Receiver Specifications

GPS receivers		RTK GPS
Accuracy (RMS)	Position	2 cm
	Velocity	0.03 m/s
Data rate		Up to 50 Hz

The yaw rate and rotational speed data of the four wheels can be obtained from the in-vehicle network and controller area network (CAN) since the vehicle is equipped with an electronic stability control (ESC) system. Tables I and II describe the specifications of on-board sensors and GPS, respectively.

The measured GPS and on-board sensor data from the probe vehicle are integrated using an information fusion algorithm. In general, the Bayesian filtering technique is widely applied to an information fusion algorithm [31]–[34]. The filtering algorithm produces their estimation of a probabilistic density function $P(x_k|Z_k)$ that describes the probability of a state x_k at time k, conditioned on the measurements Z_k up to that time. However, the filtering algorithm does not consider the measurement data after time k for the state estimation. Unlike the filtering algorithm, the fixed-interval optimal smoothing algorithm allows an information fusion algorithm to use all data before and after time k for the state estimation. The fixed-interval smoothing algorithm performs the estimation of the $P(x_k|Z_T)$ that represents the probability of a state x_k at time k, conditioned on the all finite measurements in fixed time interval, zero to T. It is possible to use the fixed-size data for the fixed-interval smoothing algorithm since the map generation algorithm performs offline after the data acquisition. The optimal smoothing algorithm uses more measurements to update the state estimate at time k than the filtering algorithm; therefore, the accuracy, continuity and reliability of the roadway estimate can be improved more than the filtering-based information fusion.

The processed data from the previous data fusion step describe roadway geometry using the huge amount of sequential points. However, the sequential point description of roadway

geometry is unsuitable for autonomous driving systems because a large memory storage is required to save the roadway map data; in addition, there is a large overhead to process all the sequential point data for application to an autonomous driving algorithm. In order to solve these problems, a mathematical road model is presented to describe the roadway geometry. Mathematical road modeling can reduce the memory storage for saving road geometry because the set of sequential roadway data is represented into compressed mathematical road model equations. In addition, the mathematical road model is more efficient for the autonomous driving algorithm such as the ego-vehicle localization, perception assistance, and road map-based path planning because it can reduce the mathematical model conversion overhead for application to the algorithm. In this paper, B-spline is used for the base mathematical road model. A gradual correction algorithm is developed and applied for road modeling in order to approximate the sequential roadway data into the B-spline. The process of the optimal smoothing and gradual correction-based road modeling is presented in Sections IV and V.

IV. Optimal Smoothing

The measurements of GPS are integrated with the data from the on-board sensors by using the fixed-interval optimal smoothing algorithm in order to improve the accuracy, continuity, and reliability of road geometry estimation. The fixed-interval optimal smoother estimates the system state at a certain time using all of the given finite set of measurements over a fixed time interval. In other words, all the measured data are used to estimate each time state. There are two types of fixed-interval optimal smoothers, namely, the forward–backward approach and the Rauch–Tung–Striebel (RTS) smoother [35]. The forward–backward smoothing method is more straightforward to understand the principle of optimal smoothing than the RTS smoother. However, the RTS smoother is used as an optimal smoothing method in this study since the RTS smoother is more computationally efficient and easier to implement.

A. System and the Measurement Model

The system model represents the vehicle motion constraint of the probe vehicle. The equation of the probe vehicle motion constraint is described in (1). The system state x_k is composed of the vehicle yaw ψ and the global positions of X and Y at discrete time k. This system state can be predicted using the previous state x_{k-1} and inputs from the rate gyro and the wheel speed on-board sensors. Noise w of the system model is assumed as white Gaussian noise with covariance Q_k, i.e.,

$$x_k = f_{k-1}(x_{k-1}, u_{k-1}, w_{k-1}), w_k \sim (0, Q_k)$$
$$\Rightarrow \begin{bmatrix} \psi_k \\ X_k \\ Y_k \end{bmatrix} = \begin{bmatrix} \psi_{k-1} + T \cdot r_{\text{gyro}} \\ X_{k-1} + T \cdot V_{\text{wheel}} \cos(\psi_{k-1}) \\ Y_{k-1} + T \cdot V_{\text{wheel}} \sin(\psi_{k-1}) \end{bmatrix} + w_{k-1}. \quad (1)$$

The measurement vector of the estimation algorithm consists of sensing data from the GPS receiver. The GPS receiver provides the course angle ψ_{GPS} and the global position of the probe vehicle X_{GPS} and Y_{GPS}. The vector has a linear relationship to the system state, as described in (2). Noise v of the measurement model is assumed to be white Gaussian noise with covariance R_k, i.e.,

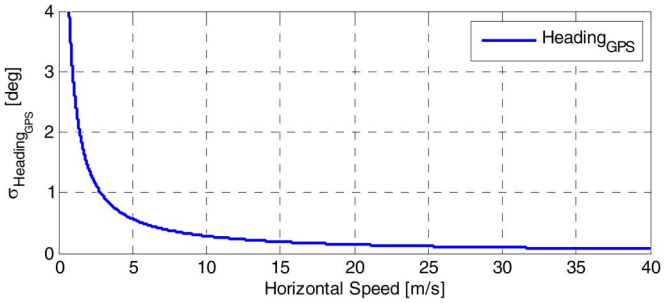

Fig. 3. Accuracy of GPS heading angle as a function of horizontal speed.

$$y_k = H_k x_k + v_k, v_k \sim (0, R_k)$$
$$\Rightarrow \begin{bmatrix} \psi_{\text{GPS}_k} \\ X_{\text{GPS}_k} \\ Y_{\text{GPS}_k} \end{bmatrix} = \begin{bmatrix} 1 & 0 & 0 \\ 0 & 1 & 0 \\ 0 & 0 & 1 \end{bmatrix} \begin{bmatrix} \psi_k \\ X_k \\ Y_k \end{bmatrix} + v_k. \quad (2)$$

GPS provides a 3-D velocity in a global coordinate. The GPS receiver velocity accuracy is about 2–5 cm/s in the horizontal plane and 4–10 cm/s in the vertical direction. The heading angle of vehicle can be calculated by taking the arctangent of the east velocity over the north velocity, as shown below

$$\psi_{\text{GPS}} = \tan^{-1}\left(V_{\text{GPS}}^{\text{east}} / V_{\text{GPS}}^{\text{north}}\right). \quad (3)$$

However, the accuracy of the heading varies with the vehicle speed since the equation of the GPS heading includes the term of velocity in the numerator. The standard deviation of the GPS heading is approximated as the standard deviation of the north velocity divided by the north velocity [36], i.e.,

$$\sigma_{\psi}^{\text{GPS}} = \tan^{-1}\left(\sigma_{\text{GPS}}^{\text{Horizontal}} / V_{\text{GPS}}^{\text{Horizontal}}\right). \quad (4)$$

Fig. 3 represents the accuracy of the heading with 5 cm/s accuracy in the horizontal plane. The error characteristic of GPS heading angle is applied to covariance R_k of the measurement model.

GPS velocity is also used to calibrate wheel speed sensors. Speed data of wheel speed sensors can contain the bias error since the radius of wheels is influenced by a change of mass of vehicle and temperature. Subsequently, the bias error of wheel speed sensors is calibrated in straight road condition using the GPS velocity that does not affect the bias error.

B. Discrete-Time Extended RTS Smoother

The linearization method used in the extended-Kalman filter is applied to the smoothing algorithm since the system model (1) of the estimation algorithm is nonlinear. The process of the discrete-time extended RTS smoother can be divided into three steps, namely, initialization, forward filter, and backward filter.

1) Initialization: At the initial time, no measurements are available to estimate the initial state and covariance. Therefore, the stochastic expected value of the initial state and the

covariance are used to initialize the state and covariance of the forward filter, as shown in (5), i.e.,

$$\hat{x}_{f0}^{+} = E(x_0)$$
$$P_{f0}^{+} = E\left[\left(x_0 - \hat{x}_{f0}^{+}\right)\left(x_0 - \hat{x}_{f0}^{+}\right)^T\right]. \tag{5}$$

2) Forward Filter: At the forward filtering step, the standard extended Kalman filter is executed for the fixed-interval time $k = 1, \ldots, N$ where N is the final time of measurement. The time update of the state and error covariance is described in (6), i.e.,

$$\hat{x}_{f,k}^{-} = f_{k-1}\left(\hat{x}_{f,k-1}^{+}, u_{k-1}, 0\right)$$
$$P_{f,k}^{-} = F_{k-1}P_{f,k-1}^{+}F_{k-1}^{T} + L_{k-1}Q_{k-1}L_{k-1}^{T}. \tag{6}$$

Since the system model is a nonlinear equation as represented in (1), the Jacobian matrices of the system model should be calculated by using (7), i.e.,

$$F_{k-1} = \left.\frac{\partial f_{k-1}}{\partial x}\right|_{\hat{x}_{f,k-1}^{+}}, \quad L_{k-1} = \left.\frac{\partial f_{k-1}}{\partial w}\right|_{\hat{x}_{f,k-1}^{+}}. \tag{7}$$

The measurement update of the state and the error covariance is performed using (8), i.e.,

$$K_{f,k} = P_{f,k}^{-}H_k^T\left(H_kP_{f,k}^{-}H_k^T + M_kR_kM_k^T\right)^{-1}$$
$$\hat{x}_{f,k}^{+} = \hat{x}_{f,k}^{-} + K_{f,k}\left[y_k - h_k\left(\hat{x}_{f,k}^{-}, 0\right)\right]$$
$$P_{f,k}^{+} = (I - K_{f,k}H_k)P_{f,k}^{-}. \tag{8}$$

If the measurement model is nonlinear, the Jacobian matrices of the measurement model are necessary, as described in (9), i.e.,

$$H_{k-1} = \left.\frac{\partial h_{k-1}}{\partial x}\right|_{\hat{x}_{f,k-1}^{-}}, \quad M_{k-1} = \left.\frac{\partial h_{k-1}}{\partial v}\right|_{\hat{x}_{f,k-1}^{-}}. \tag{9}$$

The measurement model equation (2) of the road way estimation algorithm is linear; therefore, the linearized Jacobian matrices are unnecessary for a measurement update.

GPS measurements should not be updated when the condition of GPS does not satisfy a certain threshold. The GPS condition can be deduced from the status data of GPS such as the fix quality, the number of satellites, and the horizontal dilution of precision (HDOP). All of the measured data from the GPS are neglected at the measurement update if the fix quality is not matched with desired quality (RTK fix) or the number of satellites drops below a certain threshold ($N_{\min} = 4$) or the HDOP exceeds a threshold ($H_{\max} = 5$).

3) Backward Filter: To estimate the state at time k, the forward filtering only considers the measurement before time k. However, it will improve the accuracy, reliability, and continuity of the state estimate if the measurements after time k are updated in the state estimate x_k. The RTS smoother reflects the measurements after time k to the state estimate x_k by executing backward filtering. The backward filtering performs a state update in the reverse direction for time of $k = N, \ldots, 1$, as described in (10), i.e.,

$$K_{b,k} = P_{f,k}^{+}F_k^T(P_{f,k+1}^{-})^{-1}$$
$$P_{b,k} = P_{f,k}^{+} - K_{b,k}\left(P_{f,k+1}^{-} - P_{b,k+1}\right)K_{b,k}^{T}$$
$$\hat{x}_{b,k} = \hat{x}_{f,k}^{+} + K_{b,k}\left(\hat{x}_{b,k+1} - \hat{x}_{f,k+1}^{-}\right). \tag{10}$$

The final time state of a backward filter is initialized to the end of a forward filter, as described in (11), i.e.,

$$\hat{x}_{b,N} = \hat{x}_{f,N}^{+}$$
$$P_{b,N} = P_{f,N}^{+}. \tag{11}$$

V. Road Modeling

The discrete sequential sets of the point data for road geometry are obtained from the previous optimal smoothing process. However, the roadway representation using discrete sequential sets of the point (same as the polygon method) is unsuitable for the map database of an autonomous driving system because it requires massive memory storage to save all types of the curved road geometry.

To solve the problems of the dense point description of the road maps, mathematical road modeling (based on the B-spline approximation) is applied to the map generation process. The B-spline describes the curve using a finite set of control points and knots. A *gradual correction approximation algorithm* is proposed in order to approximate the road geometry using the proper number of control points and knots. The gradual correction algorithm can represent the road geometry using a smaller set of control points and knots through adaptively arranging the control points and knots according to the approximation errors between a road model and given sequential points.

A. B-Spline Curve

A spline curve represents the sequential curve segments that are connected to create a single continuous curve. A B-spline is a type of representation of a spline curve constructed by control points, knot vectors, and basic functions. The B-spline representation of the road geometry is widely applied for road modeling because it is mathematically simpler versus the classical definition of a road that is a combination of straight lines, clothoid curves and circular curves [15], [16], [18], [19], [26]–[29]. In addition, the B-spline has many useful features to approximate road shapes such as convex hull, local modification with control points, and numerical stability. Many approximation tools developed in the field of CAD are available to apply to road modeling.

The B-spline curve $C(t)$ is described using the parametric spline equations, as shown in (12), i.e.,

$$C(t) = \sum_{j=0}^{n} N_{j,p}(t)b_j \qquad (T_{p-1} \le t \le T_{n+1}). \tag{12}$$

p is the order of the spline, $b_j (j = 0, \ldots, n)$ are the control points, and t is the parameter of the spline. The control points define the convex hull of the spline curve. Therefore, the spline curve begins from the first control point and ends at the last

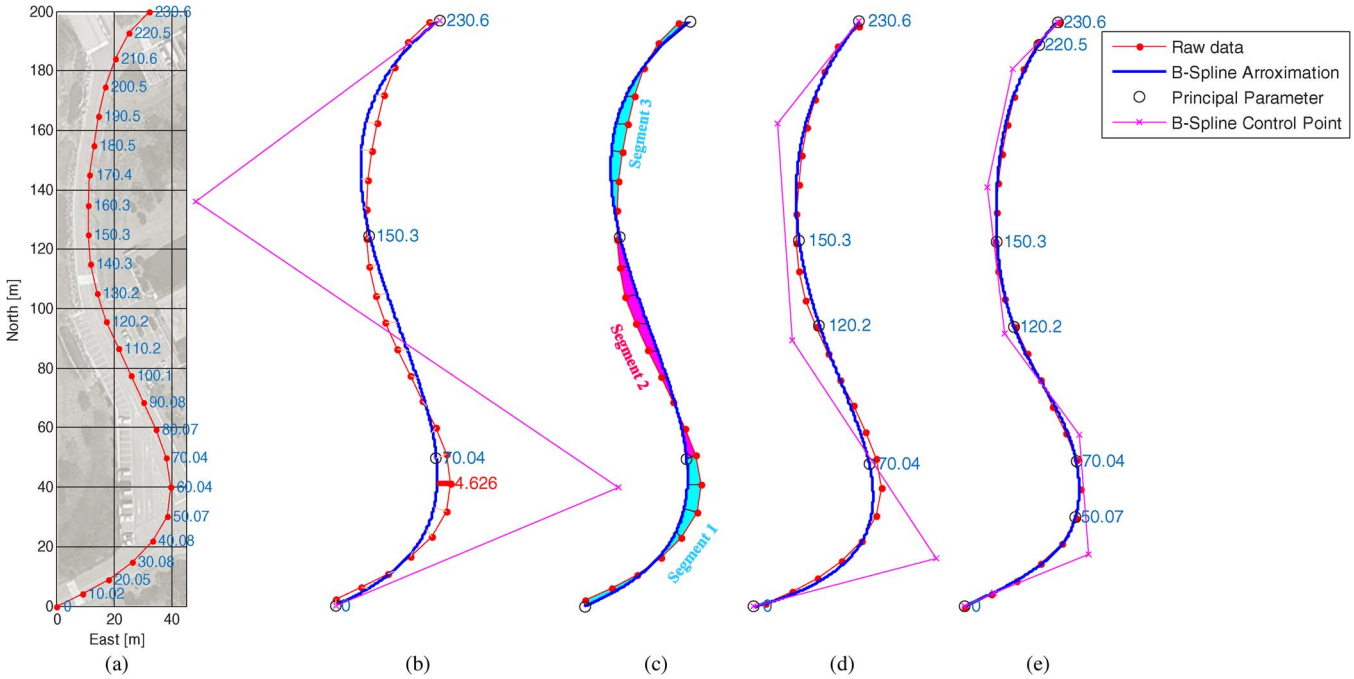

Fig. 4. Example: process of the gradual correction method for road modeling.

point, within the convex hull. The knot vector T is described as $T = [T_0, T_1, \ldots, T_{n+p-1}, T_{n+p}]$, where the elements set of T is a nondecreasing sequence of real value. To fix both the endpoints of the spline curve to the start and end of control points, b_0 and b_n, the first and last set of knots are repeated p times with the same value as follows:

$$T_0 = \cdots = T_{p-1} = t_{\text{start}},\ T_{n+1} = \cdots = T_{n+p} = t_{\text{end}} \quad (13)$$

where t_{start} and t_{end} are the parameter values of the start and endpoint of the spline, respectively.

$N_{j,p}(t)$ is the basis function of the curve with order p and can be described with the following equation:

$$N_{i,0}(t) = \begin{cases} 1 & \text{if } T_i \le t \le T_{i+1} \\ 0 & \text{otherwise} \end{cases}$$
$$N_{i,j}(t) = \frac{t - T_j}{T_{i+j} - T_i} N_{i,j-1}(t) + \frac{T_{i+j-1} - t}{T_{i+j-1} - T_{i+1}} N_{i+1,j-1}(t) \quad (14)$$

where $j = 1, 2, \ldots, p$.

B. Gradual Correction Method for Road Modeling

The processed point data of the roadway positions from the previous smoothing algorithm are fitted to a B-spline road model using a gradual correction-based road modeling algorithm. The input of the algorithm is the set of the sequential position points of the road $p_i (i = 0, \ldots, m)$, and the number of the given points should be larger than the order of the spline. The output is the B-spline road model, which has an acceptable approximation error.

Many factors of the B-spline should be appropriately determined (including the number of control points, the location of control points, order of the spline, parameterization method, and knot vectors) in order to approximate the given data points into a B-spline road model. Previous research used conventional optimization techniques to determine the B-spline factors; however, this research assumed that the number of control points is known and fixed before solving an optimization problem. The number of control points is a critical factor for roadway modeling because it determines the quality of the curve fitting and largely affects the data volume of the roadway map. The optimal number of control points can be solved using combinatorial optimization. However, this method is inappropriate to apply for practical road modeling because it will require huge amounts of time to solve the problem [10]. We adopt a gradual correction algorithm to find the number of control points and the other B-spline factors. The gradual correction algorithm provides a suboptimal solution for the number of control points and is fast enough to use for practical roadway modeling.

The process of the B-spline based road modeling takes two main steps of initialization and gradual correction. The spline parameters of all the given points are determined in the initialization step and the principal parameter vector for the B-spline approximation is initialized. In the gradual correction step, all the given position points of the roadway are iteratively approximated into the B-spline road model until the error comes within the tolerance range. The overall process of road modeling is shown through an example of the short roadway data (see Fig. 4).

1) Initialization—Spatial resampling: The result of optimal smoothing process consists of sequential trajectory points of the probe vehicle. The intervals between the sequential trajectory points may not be constant since it is difficult for the probe vehicle to acquire trajectory information at a constant speed. Therefore, spatial resampling is performed before road modeling process in order to normalize the road geometry data. The sequential points of the example are resampled at 10-m intervals (see Fig. 4).

Chord length parameterization: The parameter values of the sequential position points of the roadway $p_i(i = 0, \ldots, m)$ provided from the smoothing algorithm are computed using the chord length parameterization method. Geometrically, the chord length parameterization can be interpreted as an approximation of the arc-length parameterization. The parameter value $t_i(i = 0, \ldots, m)$ can be calculated based on the distance of the two adjacent points $\Delta_i = |p_i - p_{i-1}|$ with $\Delta_0 = 0$, as described in (15), i.e.,

$$t_i = \sum_{j=0}^{i} \Delta_j. \tag{15}$$

Fig. 4(a) describes the result of the chord length parameterization for the given 24 points of the example. The given data points are processed into the parameter based on the chord length, and the results are described in blue text.

Principal parameter vector: A B-spline road model approximation based on a gradual correction method is started from the construction of the principal parameter vector. At least the p principal parameters are required for a roadway model using the p-order B-spline. The next section introduces the reason for the minimum number of principal parameters that describes the process of a gradual correction method. The initial principal parameter vector (which contains the p principal parameter) is constructed using the evenly distributed values of the parameter for the parameterization results of a given point set, as described in (16), i.e.,

$$T_{\text{principal}} = \Big[0 \quad t_{\text{round}\left(\frac{1}{\text{p}-1}\text{m}\right)} \quad t_{\text{round}\left(\frac{2}{\text{p}-1}\text{m}\right)} \quad \cdots \quad t_{\text{round}\left(\frac{\text{p}-2}{\text{p}-1}\text{m}\right)} \quad t_m\Big] \tag{16}$$

where round(x) is the function that round element x to the nearest integer.

The order of the B-spline is 4 since the road modeling example uses the cubic B-spline to approximate the road model. The initial principal parameter vector of the example can be constructed as

$$T_{\text{principal}} = [\,0 \quad 70.04 \quad 150.3 \quad 230.6\,]. \tag{17}$$

2) Gradual Correction Algorithm: A road modeling algorithm based on gradual correction consists of three main steps (knot placement, B-spline approximation, and update principal parameter). This algorithm gradually corrects the error between the given roadway points data and the B-spline road model until it meets an acceptable tolerance range.

Knot placement: The knots of the B-spline for the road model can be determined based on the principal parameter vector. The knot vector T of the B-spline road model is calculated using an averaging technique described in (18). The techniques calculate the knot vector by averaging the principal parameter; in addition, it has an advantage to facilitate a stable approximation of the B-spline curve [37], i.e.,

$$T_{p+i-1} = \frac{1}{p-1} \sum_{j=i}^{i+p-2} \tau_j \quad (i = 1, \ldots, k-p+1). \tag{18}$$

The $\tau_j(j = 0, \ldots, k)$ are the elements of the principal parameter vector $T_{\text{principal}}$, and it consists of $k+1$ elements. The p principal parameters are necessary in order to satisfy the range constraint $k - p + 1$ since the iteration range of the averaging technique is $(i = 1, \ldots, k-p+1)$.

The knot vector of the example can be calculated by substituting (17) into (18) with a start and end knots constraint (13), i.e.,

$$T = [0 \quad 0 \quad 0 \quad 0 \quad 230.6 \quad 230.6 \quad 230.6 \quad 230.6\,]. \tag{19}$$

B-spline approximation: The previous process determined the parameters and knot vectors of the B-spline road model. Finally, the control points $b_j(j = 0, \ldots, n)$ are essential in order to complete the B-spline road approximation. In the B-spline approximation step, the control points of the B-spline are determined by minimizing the error between the given points and the approximated B-spline curve. The least-square method is applied to find the minimum error control points, as described in (20), i.e.,

$$E(b_0, \ldots, b_n) = \sum_{i=0}^{m} \|C(\bar{t}_i) - p_i\|^2. \tag{20}$$

After the B-spline approximation, the maximum error between the approximated B-spline curve and the given data points is evaluated in order to judge the finish of the gradual correction process. If the maximum error is larger than the tolerance threshold, the road modeling process goes to the next step that updates the new principal parameter. If the maximum error comes within the tolerance range, the road modeling process based on the gradual correction is finished.

Fig. 4(b) describes the result of the B-spline approximation based on least-square minimization. The black circles represent the position of the principal parameters, the purple $\times$ marks describe the location of the control points calculated from the least-square method, and the blue curve is the approximated B-spline road model. The red bar represents the maximum error of the approximation. In this example, the tolerance range was set to 1 m. The process will go to the next step since the maximum error is 4.626 m and does not satisfy the tolerance range.

Update principal parameter: A gradual improvement of the approximation of the B-spline road model is started from finding a new principal parameter. After finding the new principal parameter and executing the knot placement in (18) and the least-square minimization in (20), an improved B-spline curve can be generated. The new principal parameter is determined as a parameter of the dominant point for the given data. The dominant point is the point with the biggest impact on the approximation of the road model. The dominant point can be determined through an evaluation of the error between the road model and the given point data. The maximum error point for the given point data can be simply selected for the dominant point; however, it may have an unstable problem due to a concentration of the principal parameters and knots on the small curve region. Therefore, this study applied the segment region error for the dominant point selection to prevent the unstable problem.

The segment represents the region between each principal parameter. Fig. 4(c) describes an example of a segment, and it

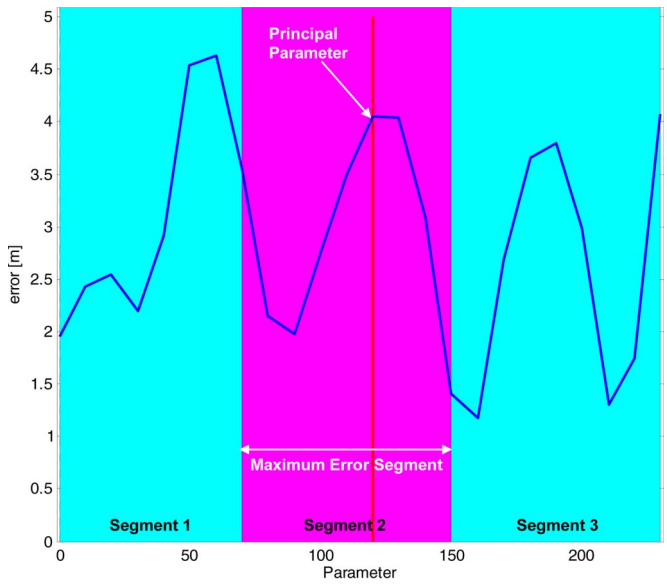

Fig. 5. Error between the B-spline approximation and given point data.

consists of three segments for the road model. The error of the segment can be calculated by using the trapezoidal method, as described in (21), i.e.,

$$\text{err}_{\text{segment}} = \sum_{i=s}^{e-1} \frac{(\text{err}_i + \text{err}_{i+1})(t_{i+1} - t_i)}{2} \tag{21}$$

$\text{err}_{\text{segment}}$ is the error of the segment, s is the start point of the segment, and e is the endpoint of the segment, and err_i is the error between the given data p_i and the road model. Fig. 5 presents the error (err_i) and segment of the example.

The dominant point for updating the principal parameter can be selected after calculating the point and segment errors $(\text{err}_i, \text{err}_{\text{segment}})$ for all given data regions. The dominant point selection is composed of two procedures: 1) the selection of maximum error segment; and 2) selection of the maximum error point. At the 1) selection of maximum error segment step, the segment for the maximum segment error $(\text{err}_{\text{segment}})$ is found. The second segment of Fig. 5 (which has a magenta color) has the maximum segment error. After finding the maximum error segment, the dominant point is determined by 2) selecting the maximum error point on the region of maximum segment error. The red line (see Fig. 5) represents the location of the selected dominant point.

The corresponding parameter of the dominant point is chosen for the new principal parameter. The new principal parameter is inserted into the principal parameter vector for the iteration of the gradual correction algorithm. The principal parameter vector of the example after the new elements insertion can be represented as

$$T_{\text{principal}} = [0 \quad 70.04 \quad 120.2 \quad 150.3 \quad 230.6]. \tag{22}$$

Using the new principal parameter, the gradually improved B-spline road model can be achieved [see Fig. 4(d)]. After the six iterations of the gradual correction algorithm, the B-spline road model, which satisfies the tolerance range (1 m), is approximated [see Fig. 4(e)].

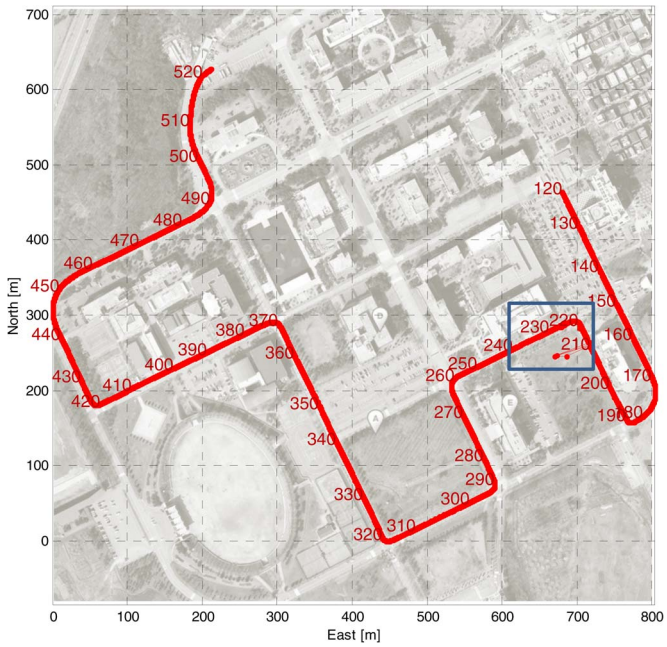

Fig. 6. Test site: Hanyang University ERICA Campus.

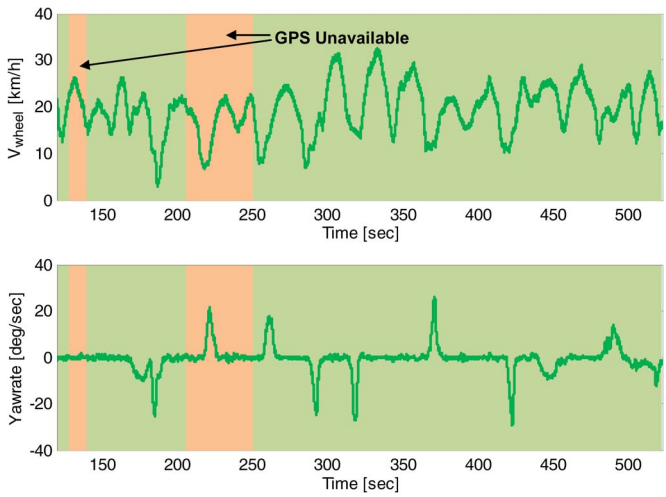

Fig. 7. Data input of the on-board sensors for the probe vehicle: Vehicle speed from the wheel speed sensors and the yaw rate from the rate gyro.

VI. Experimental Results

The experiment was performed with a probe vehicle (see Fig. 2) on the Hanyang University ERICA Campus. Fig. 6 describes the aerial photography of the test sites and the traces of the probe vehicle. The ERICA campus contains various high buildings and structures similar to urban areas; therefore, it is suitable to evaluate the performance of the sensor fusion based on the optimal smoothing method. The test site also consists of various roadway curvatures that are suitable to verify the performance of the road modeling algorithm.

A. Data Acquisition

The sequential red points (see Fig. 6) describe the position data, and the specifications from the RTK-GPS receivers are described in Table II. Fig. 7 represents the on-board sensor inputs of the probe vehicle that are the vehicle speed from the

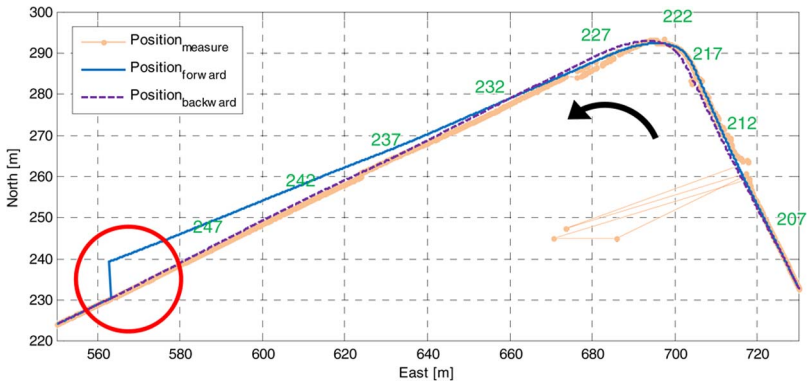

Fig. 8. Result of sensor fusion: RTS smoother-based sensor fusion of GPS and on-board sensor.

wheel speed sensors and the yaw rate from the rate gyro. The RTK-GPS receiver provides position data at centimeter-level accuracy; however, it is fragile to the external signal condition and it may offer position data that includes many errors if the signal of the GPS satellite and the RF modem is blocked by high buildings or structures. The orange color region (see Fig. 7) describes the time that the GPS is unavailable. The validation of the GPS position data is determined using the status data of a GPS receiver such as the fix quality, the number of satellites used and HDOP. An interval of 200–250 s where the box is drawn in Fig. 6 has particularly poor GPS conditions. The performance of the sensor fusion algorithm that corrects the GPS error using the on-board sensor data is evaluated in the poor GPS condition region.

B. Sensor Data Fusion With Optimal Smoothing

The GPS measurement on the poor GPS region should be integrated with the data from the on-board sensors in order to improve the accuracy, continuity, and reliability of the road geometry estimation. The RTS smoother (which is one of fixed-interval optimal smoothing algorithms) is applied to the sensor fusion algorithm. Fig. 8 describes the result of the sensor fusion using the optimal smoothing algorithm in poor GPS conditions. The orange point describes the raw position data from the GPS and the blue solid line represents the result of a forward filtering algorithm that is an Extend Kalman filter. The purple dashed line describes the result of backward filtering that is the RTS smoother. The raw data of the GPS show poor results such as severe vibration and large outliers since the test region has bad GPS signal conditions. The forward filtering algorithm (EKF) can smooth poor GPS position data; however, it has a large discrete step error at the restart point of the measurement update as described in a red circle of the figure. There are two reasons for the large discrete step error of the one-way filtering algorithm. The first reason is the drift error of the dead-reckoning process in the GPS unavailable region, and the second reason is that the state estimates are updated using only the measurement before the corresponding estimation time.

The backward filtering of the RTS smoother is applied to the result estimates of the forward filtering algorithm in order to update the state estimate using the measurement before and after the estimation time. The effect of the backward filtering can be evaluated using the standard deviation of the estimated position

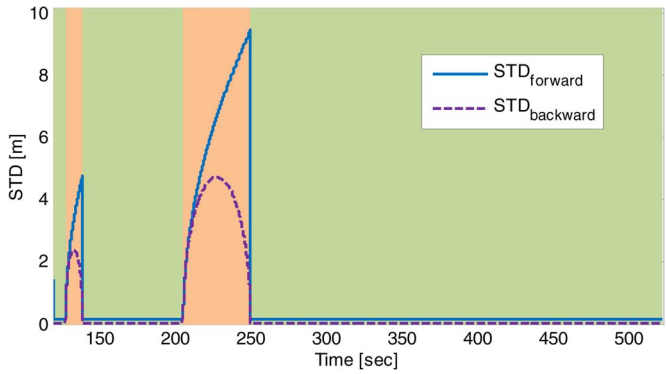

Fig. 9. Standard deviation of the position estimate.

which can be derived from the covariance matrix of both the filtering algorithms in (8) and (10). Fig. 9 represents the standard deviation of the position estimate of the forward and backward filtering. The orange color region of the figure represents the poor GPS signal conditions, and the measurement update is not performed at this region. The standard deviation of the state estimate of both filters can be only increased because there are only state predictions of the process model (6). The difference between the two filtering algorithms is the continuity and the size of the standard deviation. The standard deviation of the position estimates if the forward filtering algorithm has a large discrete correction because it only uses the measurement before the estimation time to update the state. However, the standard deviation of the backward filtering algorithm is smooth and continuous because it uses the measurement before and after the estimation time. The size of the standard deviation of the backward filtering algorithm is also smaller than the forward filter because the backward filter uses more measurements to estimate the state.

C. Road Modeling

Fig. 10 shows the B-spline road model, which is the result of the gradual correction algorithm with 0.1-m tolerance. The 2132 resampled position data from the optimal smoothing algorithm are used for the inputs of the B-spline road modeling algorithm. After the 174 iterations of the gradual correction process, the B-spline road model (which contains 181 knots and 177 control points) is achieved.

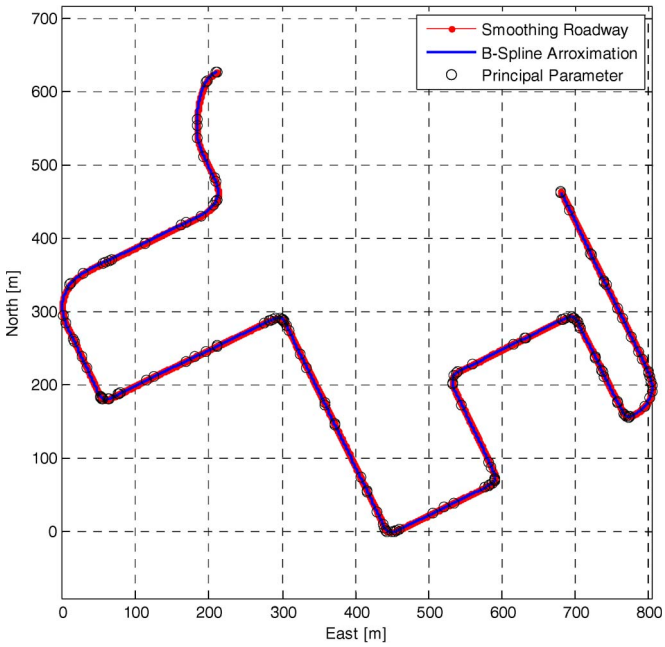

Fig. 10. Result of the B-spline road modeling-based on the gradual correction method.

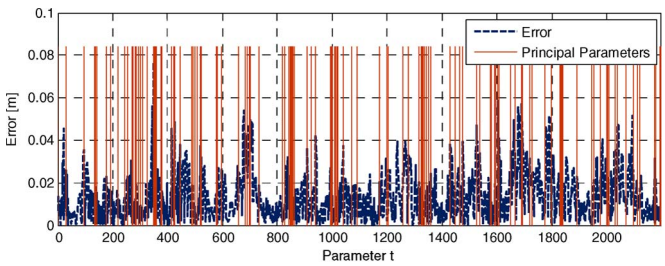

Fig. 11. Error between the road model and the optimal smoothing roadway.

The black circles (see Fig. 10) and the red line (see Fig. 11) represent the principal parameters for the gradual correction algorithm. The principal parameters are concentrated on the high curvature range; however, it is sparse in the region of a straight road because a small number of principal parameters are required to approximate the simple flat geometry. Many principal parameters are required to represent complex road geometry. The blue dashed line (see Fig. 11) describes the error between the B-spline road model and the given points data from optimal smoothing. All the errors of the B-spline approximation satisfy the 0.1-m tolerance range that is acceptable for autonomous car driving.

D. Comparison Study for Performance Evaluation of Gradual Correction Algorithm

Additional experiments were performed in the part of international F1 circuit in Yeongam, South Korea to evaluate the performance of the gradual correction algorithm compared with other road modeling methods. Fig. 12 shows the preprocessing results using the probe vehicle and RTS smoothing algorithm. The F1 circuit is suitable to evaluate the performance of the

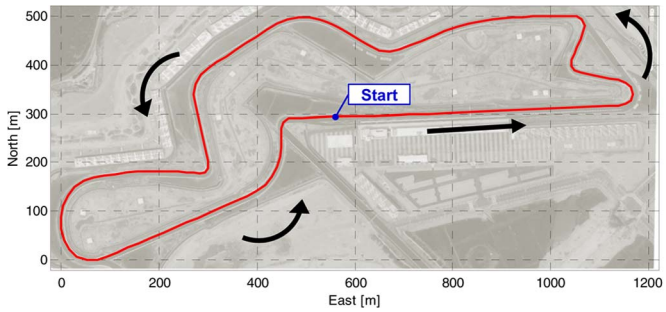

Fig. 12. Optimal smoothing results of the Yeongam international F1 circuit.

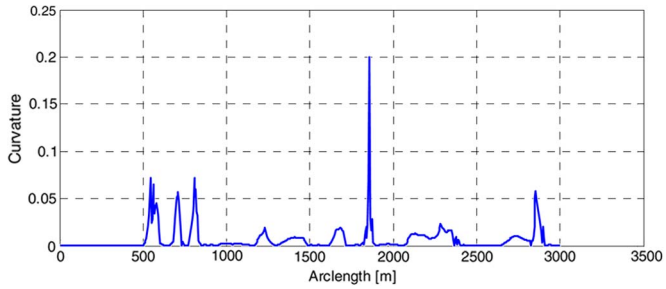

Fig. 13. Curvature of the F1 circuit with arc length.

gradual correction road modeling algorithm since it contains various road curvatures (see Fig. 13).

There are three conventional road modeling algorithms (discrete polygon, natural cubic spline, and cubic B-spline) to compare with the proposed gradual correction algorithm. The polygon method is the simplest method to model road geometry with line segments. However, a huge amount of line segments are required to achieve the desired accuracy for autonomous driving. Natural cubic spline (cubic Hermite spline) that has control points with a regular interval are used for a comparative study. The natural cubic spline is the most representative interpolating spline of the road model that passes through the regular interval control points. A cubic B-spline with knots at regular intervals is used for a comparison study. The difference between the B-spline of the gradual correction algorithm is that the knots are located at regular intervals. The clothoid curve is the best way to describe roadway geometry for autonomous driving; however, it is not convenient to utilize for autonomous car applications due to transcendental function of the clothoid curve. Therefore, this road model is excluded from the comparative study.

Road modeling based on constant number of control points: Road modeling (based on each model) was performed using the same amount of control points (30 points) in order to understand the feature of each road model. Fig. 14 shows the location of the control points and approximation results for each road model. In addition, Table III represents the approximation error of each road modeling. The polygon road model has the biggest approximation error because it represents the road geometry with the discrete line segments. The gradual correction algorithm places the knots and control points based on the geometric compliance; therefore, it has a minimum error compared with the other approaches when it has the same control points.

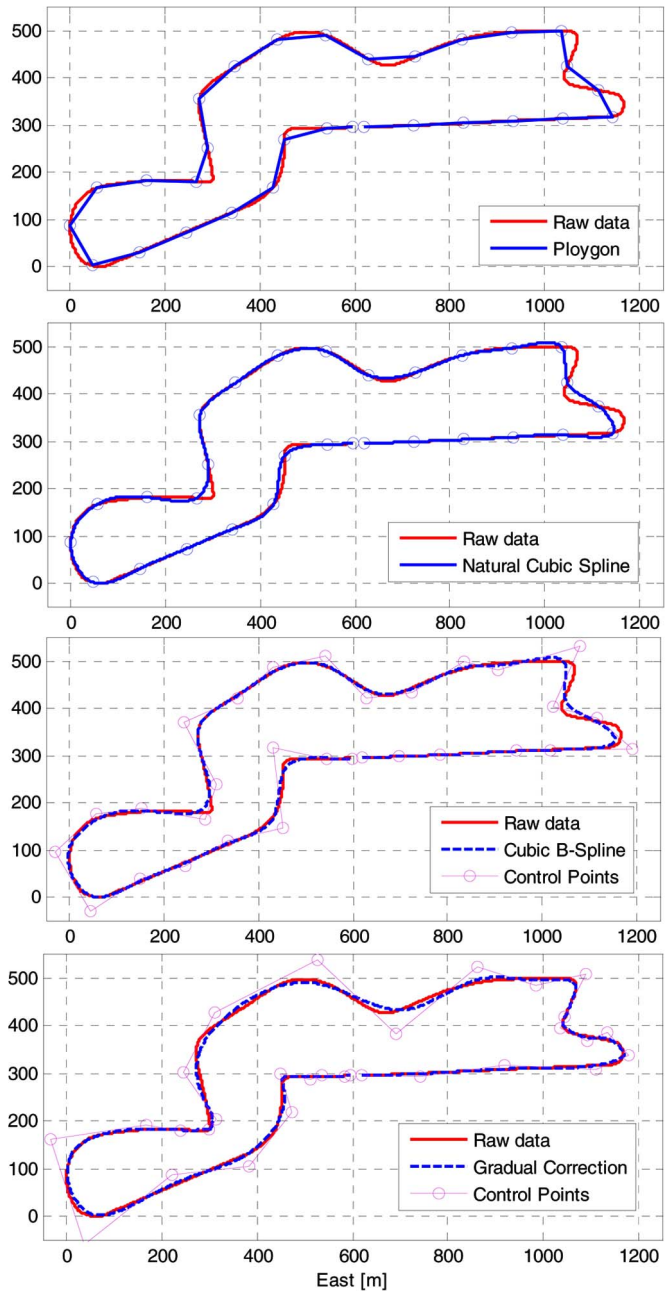

Fig. 14. Road models with a constant number of control points.

TABLE III
ERROR OF EACH ROAD MODEL WITH A CONSTANT NUMBER OF CONTROL POINTS

Polygon	Natural Cubic Spline	Cubic B-spline	Gradual Correction
34.8275 m	24.7116 m	17.5786 m	11.5293 m

Analysis of required control points to satisfy the tolerance: A gradual correction algorithm has an advantage that it can generate a high accuracy roadway model with a fewer number of control points than conventional approaches. A number of control points that satisfies the desired tolerances were analyzed for each road model in order to validate the efficiency of the gradual correction algorithm, (see Fig. 15).

The polygon road model requires the largest number of control points to present the road geometry. The natural cubic spline and cubic B-spline required a similar amount of control points to represent the desired tolerance road geometry. The regular interval spline has superior efficiency than the polygon road model. The gradual correction method can represent the desired tolerance road geometry using the smallest amount of control points. Table IV shows the required amount of control points to satisfy the tolerance of the road map for an autonomous car (0.1 m).

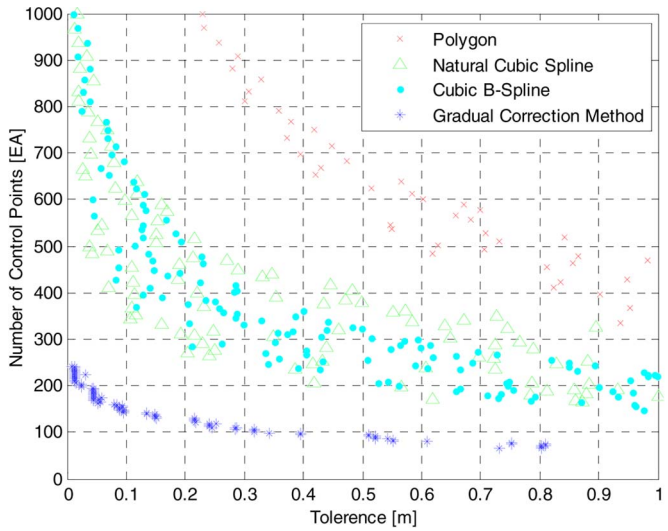

Fig. 15. Number of control points that satisfies the desired tolerances for each road model.

TABLE IV
NUMBER OF EACH ROAD MODEL WITH 0.1-m TOLERANCE

Polygon	Natural *Cubic* Spline	Cubic B-spline	Gradual Correction
5991 EA	599 EA	653 EA	149 EA

A comparison study shows that the gradual correction algorithm can reduce the number of control points to describe the road geometry. This advantage can reduce the data storage for an autonomous car and improve map data transfer communication efficiency.

VII. CONCLUSION

This paper has presented an optimal smoothing technique and a B-spline road modeling method that can generate an accurate and reliable roadway map for driving autonomous cars. A probe vehicle installed with RTK-GPS and on-board sensors (rate gyro and wheel speed sensors) measured the position data of roadway geometry. The measured data are refined through the application of a fixed-interval optimal smoothing technique (RTS smoothing) in order to improve accuracy, continuity, and reliability. A cubic B-spline is used for the road model, and a gradual correction algorithm is presented to approximate the roadway geometry into the B-spline road model. The gradual correction algorithm provides a suboptimal size of data storage to save roadway geometry data. The experimental study showed that an RTS smoother-based roadway refinement algorithm improves the accuracy, continuity, and reliability of the acquired data from a probe vehicle and road modeling based on a gradual correction algorithm that significantly compresses the size of the road geometry data.

The authors plan to extend the data processing and road modeling algorithm into a 3-D coordinate that considers further states such as the height and slope of a roadway. This paper only focuses on the preprocessing and road modeling of the roadway data. The authors intend to add road segmentation and a map database management system in order to consider a roadway network that consists of several roadway segments that covers a wide range region.

REFERENCES

[1] C. Urmson, J. Anhalt, D. Bagnell, C. Baker, R. Bittner, M. N. Clark, J. Dolan, D. Duggins, T. Galatali, C. Geyer, M. Gittleman, S. Harbaugh, M. Hebert, T. M. Howard, S. Kolski, A. Kelly, M. Likhachev, M. McNaughton, N. Miller, K. Peterson, B. Pilnick, R. Rajkumar, P. Rybski, B. Salesky, Y.-W. Seo, S. Singh, J. Snider, A. Stentz, W. R. Whittaker, Z. Wolkowicki, J. Ziglar, H. Bae, T. Brown, D. Demitrish, B. Litkouhi, J. Nickolaou, V. Sadekar, W. Zhang, J. Struble, M. Taylor, M. Darms, and D. Ferguson, "Autonomous driving in urban environments: Boss and the urban challenge," *J. Field Robot.*, vol. 25, no. 8, pp. 425–466, Aug. 2008.

[2] K. Chu, M. Lee, and M. Sunwoo, "Local path planning for off-road autonomous driving with avoidance of static obstacles," *IEEE Trans. Intell. Transp. Syst.*, vol. 13, no. 4, pp. 1599–1616, Dec. 2012.

[3] F. Chausse, J. Laneurit, and R. Chapuis, "Vehicle localization on a digital map using particles filtering," in *Proc. IEEE Intell. Veh. Symp.*, 2005, pp. 243–248.

[4] N. Suganuma and T. Uozumi, "Precise position estimation of autonomous vehicle based on map-matching," in *Proc. IEEE Intell. Veh. Symp. (IV)*, 2011, pp. 296–301.

[5] J. Levinson, M. Montemerlo, and S. Thrun, "Map-based precision vehicle localization in urban environments," in *Proceedings of Robotics: Science and Systems*. Cambridge, MA, USA: MIT Press, 2007.

[6] I. Miller, M. Campbell, and D. Huttenlocher, "Map-aided localization in sparse global positioning system environments using vision and particle filtering," *J. Field Robot.*, vol. 28, no. 5, pp. 619–643, 2011.

[7] D. Betaille and R. Toledo-Moreo, "Creating enhanced maps for lane-level vehicle navigation," *IEEE Trans. Intell. Transp. Syst.*, vol. 11, no. 4, pp. 786–798, Dec. 2010.

[8] C. Ress, A. Etemad, D. Kuck, and J. Requejo, "Electronic horizon—Providing digital map data for ADAS applications," *Madeira*, pp. 40–49, 2008.

[9] S. Durekovic and N. Smith, "Architectures of map-supported ADAS," in *Proc. IEEE Intell. Veh. Symp. (IV)*, Baden-Baden, Germany, 2011, pp. 207–211.

[10] H. Park and J. H. Lee, "B-spline curve fitting based on adaptive curve refinement using dominant points," *Comput. Aided Design*, vol. 39, no. 6, pp. 439–451, Jun. 2007.

[11] S. Schroedl, K. Wagstaff, S. Rogers, P. Langley, and C. Wilson, "Mining GPS traces for map refinement," *Data Mining Knowl. Disc.*, vol. 9, no. 1, pp. 59–87, Jul. 2004.

[12] S. Rogers, "Creating and evaluating highly accurate maps with probe vehicles," in *Proc. IEEE ITSC*, 2000, pp. 125–130.

[13] D. Ben-Arieh, S. Chang, M. Rys, and G. Zhang, "Geometric modeling of highways using global positioning system data and B-spline approximation," *J. Transp. Eng.*, vol. 130, no. 5, pp. 632–636, Sep. 2004.

[14] A. Chen, A. Ramanandan, and J. A. Farrell, "High-precision lane-level road map building for vehicle navigation," in *Proc. IEEE/ION PLANS*, 2010, pp. 1035–1042.

[15] M. Castro, L. Iglesias, R. Rodríguez-Solano, and J. A. Sánchez, "Geometric modelling of highways using global positioning system (GPS) data and spline approximation," *Transp. Res. Part C, Emerging Technol.*, vol. 14, no. 4, pp. 233–243, Aug. 2006.

[16] A. Wedel, H. Badino, C. Rabe, H. Loose, U. Franke, and D. Cremers, "B-spline modeling of road surfaces with an application to free-space estimation," *IEEE Trans. Intell. Transp. Syst.*, vol. 10, no. 4, pp. 572–583, Dec. 2009.

[17] G. Tao, K. Iwamura, and M. Koga, "Towards high accuracy road maps generation from massive GPS Traces data," in *Proc. IEEE IGARSS*, 2007, pp. 667–670.

[18] A. Schindler, G. Maier, and F. Janda, "Generation of high precision digital maps using circular arc splines," in *Proc. IEEE Intell. Veh. Symp. (IV)*, 2012, pp. 246–251.

[19] A. Schindler, G. Maier, and S. Pangerl, "Exploiting arc splines for digital maps," in *Proc. 14th Int. IEEE ITSC*, 2011, pp. 1–6.

[20] D. Betaille, R. Toledo-Moreo, and J. Laneurit, "Making an Enhanced Map for Lane Location Based Services," in *Proc. 11th Int. IEEE ITSC*, 2008, pp. 711–716.

[21] D. Bétaille, "GYROLIS: Post-processing of vehicle localization software via GPS—Gyrometer—odometer coupling," *Bull. des Laboratoires des Ponts et Chaussées*, vol. 272, pp. 75–87, 2008, GYROLIS, Logiciel de localisation de véhicule en post-traitement par couplage GPS–Gyromètre–Odomètre.

[22] D. Hahnel, D. Schulz, and W. Burgard, "Map building with mobile robots in populated environments," in *Proc. IEEE/RSJ Int. Conf. Int. Robots Syst.*, 2002, vol. 1, pp. 496–501.

[23] C. Rivadeneyra and M. Campbell, "Probabilistic multi-level maps from LIDAR data," *Int. J. Robot. Res.*, vol. 30, no. 12, pp. 1508–1526, Oct. 2011.

[24] Y.-W. Seo, C. Urmson, and D. Wettergreen, "Exploiting publicly available cartographic resources for aerial image analysis," in *Proc. 20th Int. Conf. Adv. Geogr. Inf. Syst.*, 2012, pp. 109–118.

[25] V. Gikas and J. Stratakos, "A novel geodetic engineering method for accurate and automated road/railway centerline geometry extraction based on the bearing diagram and fractal behavior," *IEEE Trans. Intell. Transp. Syst.*, vol. 13, no. 1, pp. 115–126, Mar. 2012.

[26] H. Wang, J. Kearney, and K. Atkinson, "Arc-length parameterized spline curves for real-time simulation," in *Proc. 5th Int. Conf. Curves Surfaces*, 2002, pp. 387–396.

[27] H. Wang, J. Kearney, and K. Atkinson, "Robust and efficient computation of the closest point on a spline curve," in *Proc. 5th Int. Conf. Curves Surfaces*, 2002, pp. 397–406.

[28] H. Loose and U. Franke, "B-spline-based road model for 3D lane recognition," in *Proc. IEEE 13th Int. ITSC*, Funchal, Portugal, 2010, pp. 91–98.

[29] R. Goldenthal and M. Bercovier, "Spline curve approximation and design by optimal control over the knots," *Computing*, vol. 72, no. 1/2, pp. 53–64, Apr. 2004.

[30] C. Hasberg, S. Hensel, M. Westenkirchner, and K. Bach, "Integrating spline curves in road constraint object tracking," in *Proc. 11th Int. IEEE ITSC*, Beijing, China, 2008, pp. 1009–1014.

[31] K. Jo, K. Chu, J. Kim, and M. Sunwoo, "Distributed vehicle state estimation system using information fusion of GPS and in-vehicle sensors for vehicle localization," in *Proc. 14th Int. IEEE ITSC*, 2011, pp. 2009–2014.

[32] K. Jo, K. Chu, K. Lee, and M. Sunwoo, "Integration of multiple vehicle models with an IMM filter for vehicle localization," in *Proc. IEEE Int. Veh. Symp.*, La Jolla, CA, USA, 2010, pp. 746–751.

[33] K. Jo, K. Chu, and M. Sunwoo, "Interacting multiple model filter-based sensor fusion of GPS with in-vehicle sensors for real-time vehicle positioning," *IEEE Trans. Intell. Transp. Syst.*, vol. 13, no. 1, pp. 329–343, Mar. 2012.

[34] M. Gwak, K. Jo, and M. Sunwoo, "Neural-network multiple models filter (NMM)-based position estimation system for autonomous vehicles," *Int. J. Autom. Technol.*, vol. 14, no. 2, pp. 265–274, Apr. 2013.

[35] D. Simon, *Optimal state estimation: Kalman, H [infinity] and nonlinear approaches*. Hoboken, NJ, USA: Wiley, 2006.

[36] D. M. Bevly, "Global positioning system (GPS): A low-cost velocity sensor for correcting inertial sensor errors on ground vehicles," *Trans. ASME J. Dyn. Syst. Meas. Control*, vol. 126, no. 2, pp. 255–264, Aug. 2004.

[37] L. A. Piegl and W. Tiller, *The NURBS book*. New York, NY, USA: Springer-Verlag, 1997.

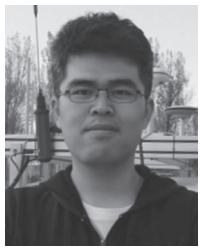

Kichun Jo (S'10) received the B.S. degree in mechanical engineering from Hanyang University, Seoul, Korea, in 2008, where he is currentxly working toward the Ph.D. degree in automotive control and electronics laboratory.

His main fields of interest are information fusion theories, distributed control systems, real-time systems, and in-vehicle networks. His current research activities include vehicle localization and system integration for an autonomous car. He has also worked on model-based embedded software development for automotive control systems.

Myoungho Sunwoo (M'81) received the B.S. degree in electrical engineering from Hanyang University, Seoul, Korea, in 1979, and the M.S. degree in electrical engineering from the University of Texas at Austin, Austin, TX USA, in 1983, and the Ph.D. degree in system engineering from Oakland University, Rochester, MI, USA, in 1990.

He joined General Motors Research (GMR) Laboratories, Warren, MI, USA, in 1985 and has worked in the area of automotive electronics and control for 28 years. During his nine-year tenure at General Motors Research (GMR), he worked on the design and development of various electronic control systems for powertrains and chassis. Since 1993, he has led research activities as a Professor with the Department of Automotive Engineering at Hanyang University, Seoul (one of the largest engineering schools in Korea). His work has focused on automotive electronics and controls (such as modeling and control of internal combustion engines, design of automotive distributed real-time control systems, intelligent autonomous vehicles, and automotive education programs). During his professional career, he has published 65 papers in international journals, presented 68 international conference papers and the holder of 25 patents. In addition, he successfully accomplished more than 50 research projects with the Korean government and automotive companies such as Hyundai, Kia, Mando, Hyundai MOBIS, and Freescale. He has continuously consulted for the Korean government and the automotive industry.

Dr. Sunwoo served as the Chairman of the steering committee for the Green Car Strategy Forum of the Ministry of the Knowledge Economy and is also a Senior Member of the National Academy of Engineering of Korea. His laboratory, i.e., ACE Lab, has been selected as a National Research Laboratory by the Korean government because of its outstanding research accomplishments. His autonomous vehicle named "A1" won the first and second National Autonomous Vehicle Competition organized by Hyundai Motor Company hosted in Korea in November 2010 and September 2012, respectively. In recognition of his distinguished achievements, he has received notable awards, such as the Grand Award of Academic-Industrial Cooperation from the Korean Academic-Industrial Foundation, the Best Scientist/Engineer Award of the Month from the Korean Ministry of Science and Technology, and the Award for Technology Innovation from the Prime Minister of Korea.